Incongruence between morphological and molecular diversity in Coxicerberus fukudai (Ito, 1974) (Isopoda: Microcerberidea) from East Asia

Article *in* Journal of Crustacean Biology · March 2018

DOI: 10.1093/jcbiol/ruy002

CITATIONS
2

READS
335

4 authors:

Jeongho Kim
Hanyang University
13 PUBLICATIONS **5** CITATIONS
SEE PROFILE

Marina Malyutina
National Scientific Center of Marine Biology
135 PUBLICATIONS **2,649** CITATIONS
SEE PROFILE

Wonchoel Lee
Hanyang University
215 PUBLICATIONS **1,362** CITATIONS
SEE PROFILE

Ivana Karanovic
Hanyang University
148 PUBLICATIONS **1,389** CITATIONS
SEE PROFILE

Journal of Crustacean Biology

The Crustacean Society

Journal of
Crustacean Biology

Journal of Crustacean Biology (2018) 1–14. doi:10.1093/jcbiol/ruy002

Incongruence between morphological and molecular diversity in *Coxicerberus fukudai* (Ito, 1974) (Isopoda: Microcerberidea) from East Asia

Jeongho Kim[1], Marina Malyutina[3], Wonchoel Lee[1] and Ivana Karanovic[1,2]

[1]*Department of Life science, Hanyang University, Seoul, Republic of Korea;*
[2]*Institute for Marine and Antarctic Studies, University of Tasmania, Hobart, Tasmania, 7001, Australia; and*
[3]*Institute of Marine Biology, Far-Eastern Branch of Russian Academy of Sciences, Vladivostok, Russian Federation*

Correspondence: Wonchoel Lee; e-mail: wlee@hanyang.ac.kr

(Received 27 June 2017; accepted 19 January 2018)

ABSTRACT

Coxicerberus fukudai (Ito, 1974) (Isopoda) is redescribed from Korean and Japanese localities. Molecular analysis based on two mitochondrial markers (mtCOI and Cytb) of the studied populations shows two diverged lineages, reflected in high (10.5% and 9.5%) pairwise differences and high haplotype diversity. One of the clades is shared by Korean and Japanese populations with little divergence rate (0.02% and 0.03%), and another is only found in Korea. We failed to find any consistent morphological differences across the examined populations, probably indicating the existence of cryptic species. We also examined the possible influence of the endosymbiotic bacterium *Wolbachia* on the haplotype diversity. Infection with the bacterium shows a distinct distribution pattern, with all the southern Korea populations being infected, whereas the northern populations are not.

Key Words: cryptic species, haplotype network, marine interstitial, phylogeny, *Wolbachia*

INTRODUCTION

Many interstitial species of isopods belonging to the family Microcerberidae Karaman, 1933 have been recorded worldwide. Although not much is known about the ecology of the family, Albuquerque *et al.* (2009) indicated a high degree of euryhalinity and eurythermy (between 10‰ to 60‰ and 10 °C to 30 °C, respectively) for at least one of the species. Due to the similarity in their general appearance, microcerbrids were considered members of the superfamily Anthuroidea until Lang (1961) established the suborder Microcerberidea based on the unique shape of the mouthparts and claws of the pereopods. Lang still considered Microcerberidea and Anthuroidea as closely related. Wägele (1982) corroborated their distant relationship with the morphology of the mandible, appendix masculina of male pleopod II, and uropods. The appendix masculina of anthurid isopods has a relatively simple structure, having a medial rod inserted on the apex of the endopod of pleopod II. The entire appendix masculina in Microcerberidea, however, is a highly specialized copulatory organ in the majority of the species (Wägele, 1982). Wägele (1983) divided the suborder Asellota into two lineages, Janiroidea and Aselloidea, based on the morphology of all pleopods. Microcerberidae was originally placed in the latter lineage, but Brusca & Wilson (1991) placed it in a separate group, Microcerberidea, together with Atlantasellidae.

Coxicerberus Wägele, Voelz & McArthur, 1995 is one of the largest of the seven Microcerberidae genera, comprising 33 described species (Boyko *et al.*, 2008). It was erected to include a few species of *Microcerberus* Karaman, 1933, based mainly on the pointed coxae of pereonites, a biramous pleopod III, and a short uropod exopod. The majority of the species of *Coxicerberus* inhabit marine and freshwater interstitial environments throughout tropical and temperate regions (Ito, 1974). *Coxicerberus* is morphologically homogeneous, and species delineation requires detailed observation of minute characters, including the male appendix masculina in pleopod II. Baldari & Argano (1984) pointed out an interspecific variability of this structure in *Microcerberus*, and divided the genus into four species groups (*remenai*, *anfidincus*, *stygius*, and *mirabilis*) based on the form of the male pleopod II. Many species of the *remenai* and *mirabilis* groups showing a relatively complex structure of the male pleopod II were transferred to *Coxicerberus* by Wägele *et al.* (1995). *Coxicerberus* is the only microcerberid genus known from East Asia, with three species described so far from Japan, *C. kiiensis* (Nunomura, 1973), *C. fukudai* (Ito, 1974), and *C. boninensis*, (Ito, 1975).

We discovered *C. fukadai* during a survey on the beach interstitial fauna along the east coast of Korea and from one locality in Hokkaido, Japan, the type locality. Microcerberidss are much smaller (about 0.5–1.2 mm) and less mobile than other isopods,

and have preference for the interstitial environment, so they are difficult to find. Several microcerberid species even have a wider distribution, with *C. abbotti* (Lang, 1961) found along the North American Pacific coast, *C. remanei* (Chappuis & Delamare-Deboutteville, 1954) across the Mediterranean and the Portuguese Atlantic coast, and *C. anfindicus* (Messana, Argano & Baldari, 1978) from Somalia and the Maldives (Baldari & Argano, 1984). Many studies using molecular markers have found distinct clades among the superficially homogeneous species of isopods that show a wide distribution (Held & Wägele, 2005; Raupach *et al.*, 2007, 2014; Markow & Pfeiler, 2010; Varela & Haye, 2012; Yin *et al.*, 2013; Lee *et al.*, 2014).

Species delimitation based on molecular data revolves around the degree of molecular differences ("bar code gap" in mtCOI) and depends largely on the group in question and the gene segment. Among isopods, Markow & Pfeiler (2010) reported a large spectrum of the interspecific p-distances in *Ligia* Fabricius, 1798, ranging from 14.9% to 30.3%. Varela & Haye (2012) discovered a cryptic species in the *Excirolana braziliensis* Richardson, 1912 complex along the coast of Chile based on 17%–19% p-distances, whereas Brix *et al.* (2014) found five distinct lineages within *Chelator insignis* (Hansen, 1916), with over 20% of uncorrected p-distance. Khalaji-Pirbalouty & Raupach (2014) applied the K2P distance method and found interspecific distances between four species of *Cymodoce* Leach, 1814, ranging from 3.93% to 23.37%. Raupach *et al.* (2015) identified an average intraspecific K2P distance of 3.19% in populations of *Astacilla intermedia* (Goodsir, 1841), with provisional cryptic species indicated even with such small values.

The aim of this study was to investigate the morphological and molecular diversity of *C. fukudai* from Korea and Japan. We choose two mitochondrial markers (mtCOI and Cytb) and one nuclear marker (hypervariable V7 expansion region of 18S rDNA). The latter marker was chosen to study a potential influence of the *Wolbachia* infection on haplotype diversity. Genetic variability of mitochondrial DNA can occasionally be influenced by maternally inherited endosymbionts, particularly *Wolbachia* α-proteobacteria, which are known to cause cytoplasmic incompatibility and linkage disequilibrium, reducing mitochondrial DNA diversity or increasing the substitution rates in various arthropods, including isopods (Shoemaker *et al.*, 2004; Hurst & Jiggins, 2005; Xiao *et al.*, 2012).

MATERIAL AND METHODS

Collection and processing of specimens

Information of specimens used for the study is summarized in Supplementary material Table S1. Sampling was conducted on eleven sandy beaches along the east coast of Korea (Fig. 1). An additional sample was collected from Hamakoshimizu, Hokkaido, Japan (Fig. 1H). Samples were collected by the Karaman-Chappuis method (Chappuis, 1942), and the water was filtered with the hand net (mesh size 46 μm). All collected materials were immediately preserved in 99% ethanol.

Sorting and dissecting of specimens were done using a dissecting microscope, the line drawings were made using a Leica DM2500 (Leica, Wetzlar, Germany) compound microscope equipped with a camera lucida. All newly collected materials were deposited in the collection of the National Institute of Biological Resources (NIBR), Incheon, Korea. Measurements were done by following the method of Riehl & Brandt (2010), using the distance measurement tools of Adobe Acrobat X Professional from the dorsal view of the line drawings. The appendage to length ratios were given in distal to proximal order, excluding seta; body length ratios in anteromedial to posteromedial point order excluding appendages. Total body length was measured fusing the largest female specimens. The terminology used was largely based on Ito (1974) and Wägele *et al.* (1995), with several modifications.

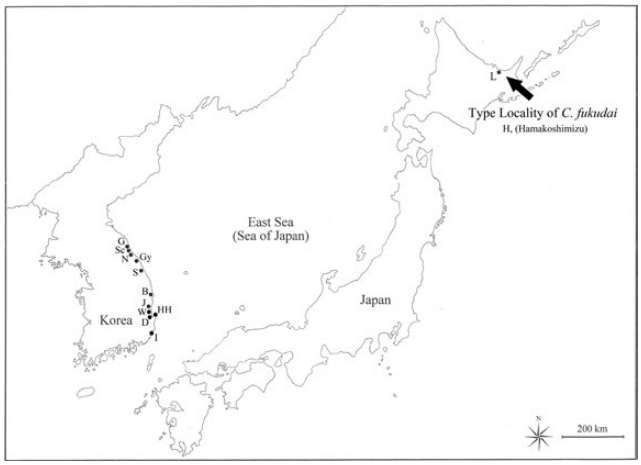

Figure 1. Sampling locations in Korea and Japan: Gazin (Ga), Sokcho (Sc), Naksan (N), Gyeongpo (Gy), Samcheok (S), Byeonggok (B), Jangsa (J), Wolpo (W), Dogu (D), Heunghan (HH), Imrang (I), Hamakoshimizu (H), Japan (type locality of *Coxicerberu fukudai*).

Two adult males and two adult females were randomly selected from the samples and prepared for SEM analysis. Each specimen was transferred to isoamyl acetate for 20 min and dried in a critical-point dryer (Hitachi E-1010; Hitachi, Tokyo, Japan). Dried specimens were mounted on a SEM stub coated with gold using a sputter coater to a thickness of 15–30 nm. The coated specimens were examined and photographed with a Hitachi S-3400 scanning electron microscope at Chungang University, Seoul, Korea. The type series of *Coxicerberus fukudai* (Ito, 1974) were borrowed from Seto Marine Biological Laboratory, Shirahama, Japan for comparing with the collected specimens.

PCR amplification

Before amplification, specimens were transferred into distilled water for 20 min to remove ethanol and pulverized with a glass stick. Whole specimens were used to isolate genomic DNA with the aid of the LaboPassTM Kit (Cosmo, Seoul, Korea) following the manufacturer's protocols. A fragment of the mtCOI gene was amplified through polymerase chain reaction (PCR) using a PCR primer (Bioneer, Dajeon, Korea) in TaKaRa PCR thermal cycler (TaKaRa Bio, Kusatsu, Japan). The degenerated Folmer primer pair (Folmer *et al.*, 1994), Maxillo FOR (5'-CWAAYCATAAAGAYATTGGNAC-3'), and Maxillo REV (5' -ACTTCAGGRTGNCCAAARAAY-3') designed by Y.-H. Lee (Korea Institute of Ocean Science & Technology, Ansan), were used. For Cytb, UCYTB151F (5'-TGTGGRGCNACYGTWATYACTAA-3') and UCYTB270R (5'- AANAGGAARTAYCAYTCNGGYTG-3') primers (Merritt *et al.*, 1998) were used. The hypervariable V7 region of the nuclear 18S rRNA gene, which is known to vary between closely related species (Raupach *et al.*, 2010; 2014), was used. This region was amplified with LoV7F (5'-GGGACCACCAGGAGTG-3') and LoV7R (5'-GGCCCAGAACATCTAAGG-3'). The amplification protocol for mtCOI consisted of initial denaturation at 94 °C for 5 min, 40 cycles of denaturation at 94 °C for 30 sec, annealing at 42 °C for 2 min, extension at 72 °C for 1 min, final extension at 72 °C for 10 min, and storing at 4 °C. The protocol for Cytb consisted of the initial denaturation at 94 °C for 5 min, 40 cycles of denaturation at 94 °C for 30 sec, annealing at 42 °C for 2 min, extension at 72 °C for 1 min, and final extension at 72 °C for 10 min, and storing at 4 °C. The PCR amplification of the V7 region of 18S gene was undertaken by following Raupach *et al.*, (2014). The presence of *Wolbachia* was investigated using the wsp gene region that contains a highly variable 575–625bp portion encoding the bacterial surface protein; 40 genomic DNA from all studied localities were used

and amplified using the primers and protocols of Braig *et al.* (1998), Zhou *et al.* (1998), and Cordaux *et al.* (2001). The same isolates used to obtain mitochondrial and nuclear markers were used to test for the presence of *Wolbachia*. The PCR products were purified for sequencing reactions using the Labopass PCR Purification Kit (Cosmo, Seoul, Korea) following the instructions of the manufacturer. DNA was sequenced on an ABI automatic capillary sequencer (Macrogen, Seoul, Korea) using the same set of primers.

Phylogeny and haplotype analysis

All obtained sequences were confirmed with BLAST search (Altschul *et al.*, 1990) and visualized using Finch TV, version1.4.0 (http://www.geospiza.com/Products/finchtv.shtml). Each sequence was tested for the quality of signal and sites with possible low resolution, and corrected by comparing forward and reverse strands. Sequences were imported into MEGA 7 (Kumar *et al.*, 2016) and aligned with Clustal W (Thompson *et al.*, 1994) with MEGA default parameters. After the alignment each sequence was checked for potential stop codons with ORF finder on the NCBI website (http://www.ncbi.nlm.nih.gov/projects/gorf/) using the invertebrate mitochondrial code. Newly obtained sequences are publicly available on GenBank (Supplementary material Table S1). The K2P model (Kimura, 1980) implemented in MEGA 7 was used to calculate the pairwise distances between sequences. For the best-fit evolutionary model program jModelTest 2.1.6 (Guindon & Gascuel, 2003; Darriba *et al.* 2012) was used with Akaike Information Criterion (Akaike, 1974; Yamaoka *et al.*, 1978; Hurvitch & Tsai, 1989). The mtCOI phylogram was finally rooted with the two isopod sequences from the gene bank: *Proasellus parvulus* (Sket, 1960) YCD534, and *Asellus aquaticus* (Linnaeus, 1758) FJ749279, whereas the Cytb phylogram was unrooted. The following phylogenetic analyses were performed: maximum-likelihood (ML) using MEGA 7 (Kumar *et al.*, 2016) and Bayesian inference in MrBayes (Huelsenbeck *et al.*, 2001; Ronquist & Huelsenbeck, 2003; Ronquist *et al.*, 2012). Maximum likelihood was performed using the best fit evolutionary model with partial deletion (95%), Nearest-neighbor-interchange as the heuristic search method, and the initial phylogram were created automatically (Default-NJ/BioNJ). Non-parametric bootstraps were calculated based on 1,000 pseudoreplicates (Felsenstein, 1985). Bayesian analyses ran with four chains simultaneously for two million generations in two independent runs, sampling phylograms every 200 generations. Of the four chains, three were heated and one was cold, the temperature value ("temp" command in MrBayes) was 0.1 (default option). The results were summarized and phylograms from each MrBayes run were combined with the default 25% burn-in. A > 50% posterior probability consensus phylogram was constructed from the remaining ones.

Haplotype diversity (Rozas & Rozas, 1999), nucleotide diversity (π) (defined as the average number of pairwise nucleotide differences (Tajima, 1983; Nei, 1987), and their standard deviations), DnaSP 5.10 (Librado & Rozas, 2009) were used in the statistical estimation of the number of haplotypes. The TCS algorithm implemented in PopART (Clement *et al.*, 2000; Leigh & Bryant, 2015) was used to visualize the haplotype network for mtCOI and Cytb sequences.

SYSTEMATICS

Order Isopoda Latreille, 1817

Suborder Microcerberidea Lang, 1961

Family Microcerberidae Karaman, 1933

Genus *Coxicerberus* Wägele, Voelz & McArthur, 1995

Coxicerberus Wägele, Voelz & McArthur, 1995: 741. – Albuquerque *et al.*, 2009: 1179.

Type species: *Coxicerberus mirabilis* (Chappuis & Delamare-Deboutteville, 1956).

Diagnosis (modified from Wägele *et al.*, 1995): Colorless body, cylindrical, approximately 10× longer than wide. Cephalon, rectangular, no visual organ, anterior margin smooth, without rostrum. Tergites of pereonites II-IV with one pair of coxae pointed distally. Pleopod I absent. Male plepod II with rectangular protopod, minute round exopod, apically bifid or trifid, elongated endopod of varying shapes. Pleopod III uniramous. Pleopod IV covered by pleopod III, biramous, without articulation. Uropod with globular protopod, minute exopod, longer endopod, tapering distally.

Remarks: The East Asian species of *Coxicerberus* share a similar morphology with a few North American congeners despite the geographical distance. Nunomura (1973) and Ito (1974) found that the morphology of male pleopod II of *C. kiiensis* and of *C. fukudai* is very similar to that of *C. abbotti*. These three species also share a similar armature (spinular rows) of the medial margin of the pleopod II endopod, a pointed distal tip of the endopod of pleopod II, and have distally elongated appendix masculina. *Coxicerberus boninensis* Ito, 1975, described from the isolated Bonin Islands, is morphologically very similar to *C. mexicanus* (Pennak, 1958) by having a five-segmented antennula and similar antennal flagellum and a general appearance of the male pleopod II. Distomedially elongated spines on the endopod of pleopod II is their synapomorphic character. These morphological similarities are noteworthy considering the wide geographical distance and the weak mobility of *Coxicerberus*. Baldari & Argano (1984) also recognized this phenomenon and classified these two cases of morphological similarities into the *remanei* and *mirabilis* groups, respectively. No explanations on the phylogenetic relationships and biogeography of each group were given.

Coxicerberus fukudai (Ito, 1974)
(Figs. 2–13)

Microcerberus fukudai Ito, 1974: 339; 1975: 126. – Baldari & Argano, 1984: 116.

Type locality: Hamakoshimizu, Hokkaido, Japan.

Material examined: One adult male (NIBRIV0000813453, 0.79 mm) dissected on four slides, one adult male (NIBRIV0000813454; 0.76 mm) on four slides, and one adult female (NIBRIV0000813455; 1.02 mm) on three slides, Sokcho, Korea (38°11'14.2"N 128°36'22.0"E). One adult female (NIBRIV0000813456; 1.06 mm) dissected on one slide and two adult males (NIBRIV0000813457; 0.81mm, 0.78 mm) on one slide, Gazin, Korea (38°37'29.5"N 128°50'92.1"E). One adult, undissected male on one slide (NIBRIV0000813458; 0.72mm), Naksan, Korea (38°6'34.15"N 128°38'48.2"E). Two adult, undissected males on one slide (NIBRIV0000813459; 0.71 mm, 0.74 mm), Gyeongpo, Korea (37°48'4.74"N 128°54'13.54"E). Two adult, undissected males on one slide (NIBRIV0000813460; 0.73 mm, 0.7 mm), Samcheock, Korea (37°27'57.2"N 128°10'20.05"E). Two adult, undissected males on one slide (NIBRIV0000813461; 0.76 mm, 0.78 mm), Wolpo (36°16'39.26"N 129°22'43.07"E). Two adult males dissected on one slide (NIBRIV0000813462; 0.74 mm, 0.73 mm), Heunghan, Korea (36°02'36.46"N 129°49'85.00"E). Two adult males dissected on one slide (NIBRIV0000813463; 0.82 mm, 0.8 mm), Imrang, Korea (35°31'86.31"N 129°26'41.18"E). One adult, undissected female on one slide (NIBRIV0000813464; 0.98 mm), Hamakoshimizu, Japan (43°56'05.4"N 144°27'15.8"E). Twenty-five males (NIBRIV0000813465), Byeonggok, Korea (36°35'18.83"N 129°24'37.15"E) and 25 males (NIBRIV0000813466), Jangsa, Korea (36°16'39.26"N 129°22'43.07"E) in 70% ethanol. Two males and two females (NIBRIV0000813467), Sokcho, Korea (38°11'14.2"N 128°36'22.0"E) used for SEM.

Diagnosis (male): Antennula with 6 articles; antenna with 6 flagellar articles; cephalon 1.5× longer than wide, with 7 pairs of simple setae; article V of maxilliped tapering distally, with 3 distal stout setae, 2 subdistal small setae, 2 spinular rows; pereonite I 1.7× longer than cephalon, anterior margin with 4 simple setae; pleotelson 1.15× longer than wide, 1.4× longer than pleonite II; penial papillae consisting of 2 trapezoidal lobes, with distomedial groove; endopod of pleopod II tapering distally, with incurved lateral margin, medial margin covered by several spinular lows, with long appendix masculina, length reaching to almost end of pleotelson.

Description (based on male NIBRIV0000813453, 0.79mm)

Body (Fig. 2, 3A) with pereonite I 1.7× longer than cephalon, anterior margin with 4 simple setae, as broad as cephalon, tapering posteriorly, lateral margin with 2 simple setae; pereonites II (see Fig. 3A) subequal, as wide as pereonite I posteriorly, 1.25× longer than wide, pereonite II–IV (see Fig. 2A & 3A) tergite with pair of coxae and main tergal plate, anteromedian margin of tergal plate with medial incision with pair of setae, coxae pointed distally with minute distal spinules, pair of small setae on distomedial margin, pair of setae on lateral margin; pereonites V–VII (see Fig. 2A) subequal to cephalon in width, length; larger than preceding pereonites, with pair of setae on dorsal margin, tergite simple, no accessory plate, longitudinal crevice on medial margin, lateral margins with pair of setae, each. with pleonite I and II subequal in size, shape; about half as long as pereonites V–VII, lateral margin with pair of setae, dorsal surface with 2 simple setae; pleotelson I 1.5× longer than wide, 1.4× longer than pleonite II, dorsal surface with 2 pairs of setae, lateral margin slightly convex with pair of setae, posteroventral margin with 2 pairs of simple setae (see Fig. 7A).

Cephalon (Fig. 3A) 1.5× longer than wide, 0.1× body length, lateral margins with 5 pairs of simple setae each, dorsal surface with 2 pairs of setae, pair of incisions on dorsoposterior margin.

Antennula (Fig. 3B) directed anterolaterally, 0.13× as long as body length, consisting of 3 peduncular, 3 flagellar articles; article I largest, 1.4× longer than wide, with broom seta, simple seta of same length, shorter distolateral setae; article II 0.7× as long as article I, tapering distally, proximolateral margin with 3 broom setae; article III 0.6× as wide as article II, 1.4× longer than wide, with 2 simple distomedial setae; article IV 0.6× as long as article III, with short seta, broom seta on distomedial corner; article V as long as article III, with simple distomedial seta; article VI 1.8× longer than wide, with aesthetasc, one broom seta, 3 simple setae.

Antenna (Fig. 3C) with 6 peduncular, 6 flagellar articles; 1.8× longer than antennula, 0.24× body length, peduncle 0.75× total length; article I triangular, with ventral seta; article II 0.36× wider than long, with ventral seta; article III 1.7× longer than wide, tapering distally, with 2 setae on proximolateral edge, 2 ventromedial setae, medial edge with subproximal protrusion; article IV broadening distally, with 3 setae; article V 2× longer than wide, lateral margin slightly produced in midlength, with short broom seta plus 3 longer, simple setae; medial margin with 3 setae; article VI 1.2× longer than article V 2.5× wider, lateral margin with simple seta, 3 short broom setae on distal half, distal broom seta subequal to article in length, medial margin with simple subproximal seta, one broom seta, 5 simple subdistal setae of different

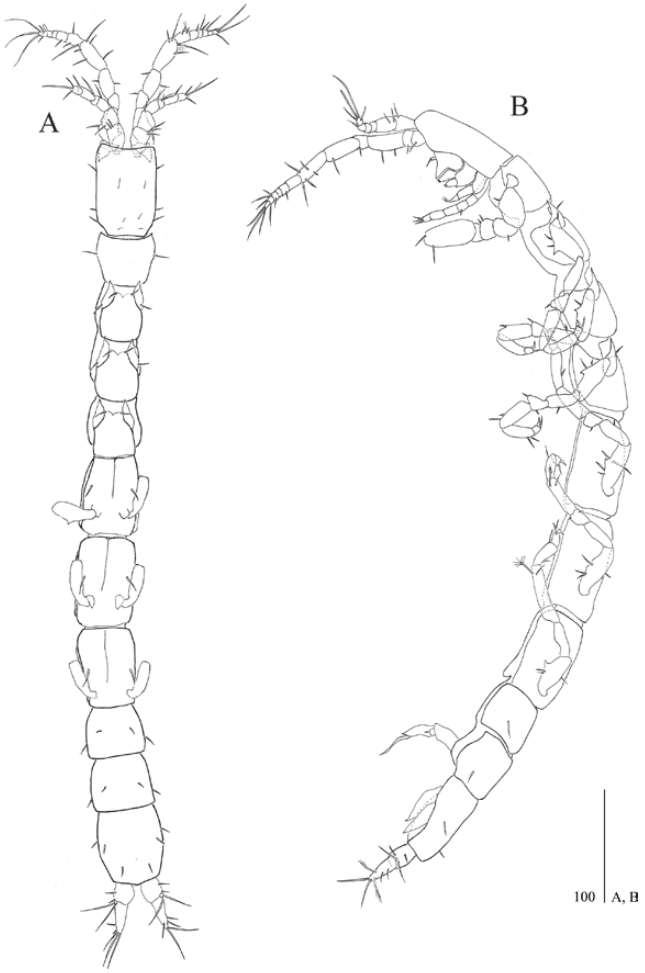

Figure 2. *Coxicerberus fukudai*, male, habitus; dorsal (**A**); lateral (**B**). Scale bar 100 µm, 600×.

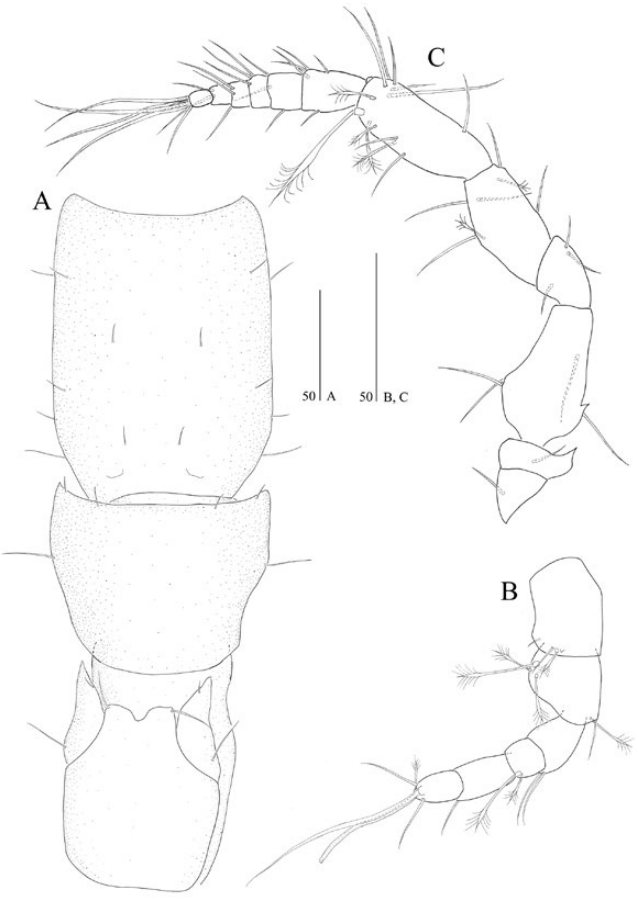

Figure 3. *Coxicerberus fukudai*, male: cephalon, pereonites I and II dorsal (**A**); antennula, dorsal (**B**); antenna, dorsal (**C**). Scale bar: 50 µm, 1000×.

lengths; flagellum tapering distally, with 6 articles; flagellar article I 1.6× longer than wide, with 5 simple setae (see Fig. 8A); article II as long as wide, with 3 setae distally; each article III, IV half as long as article II, wider than long, with 3 setae, respectively; articles V, VI slightly narrower than preceding articles; article V with 2 distal setae, article VI with 5 distal setae, one short, 4 nearly as long as flagellum.

Mandible (Fig. 4A–D) robust, curved inwardly; pars incisiva of mandibles with 4 cusps, median one largest; lacinia mobilis of left mandible smaller than pars incisiva, tapering proximally, distal margin serrated, 2 pinnate setae located below lacinia mobilis; pars molaris tapering distally without apical setae; lacinia mobilis of right mandible with 4 cusps, slightly larger than pars incisiva, with 3 pinnate setae; mandibular palp, article I, elongated, 2.4× longer than wide, attached on distolateral projection, with apical seta, 2.7× as long as article.

Maxilla (Fig. 4E) protopod with 2 distal rami, both rami cylindrical, subequal in length; with stout pinnate seta, respectively.

Maxillula (Fig. 4F) outer lobe with 8 robust setae on distal margin, some bifid, some pinnate; inner lobe about half as long and wide as outer endite, with 3 short apical setae.

Maxilliped (Fig. 5A) without epipod, basis, 2.1× longer than wide with spinular row on ventrolateral side, endite, 0.25× wider than basis, with 2 spinular rows on medial margin, distal margin narrow, rounded, reaching 0.35× medial length of palp article I, with minute distal seta; palp slightly curved inwardly, much longer than basis, tapering distally; article I with short distomedial seta; article II broadest, 1.2× as wide as article III, slightly longer medially than article I, with 2 setae on distomedial corner, both articles with spinular row on distolateral area, respectively; article III longest, ratios of middle length of articles II–V to article I 0.8, 1.3, 1.2, 0.85; article III subequal to article II medially, 1.7× as long as article II laterally, slightly narrower, with distomedial seta, spinular row on proximolateral area; article IV with 2 distomedial setae; article V tapering distally, with distally 3 stout setae, 1.5× as long as article, 2 subdistal small setae, with 2 spinular rows medially.

Pereopod I (Fig. 5B) inserted on pereonite I anterolaterally, subchelate; basis, robust, length ratios of dactylus to basis: 0.7, 0.5, 0.6, 1.65, 0.75; basis, 1.52× longer than wide, with seta on middle anterior edge; ischium, 1.7× longer than wide, with ventral seta plus 4 spinular rows laterally; merus, 1.1× longer than wide, with spinular row on surface, 2 setae dorsally, 3 setae ventrally; carpus nearly triangular, 1.05× longer than wide, with 6 small setae along ventral margin, 3 long distoventral setae, 2 spinular rows on subventral margin; propodus, 2.2× longer than wide, tapering distally with 4 simple subdistal setae, ventral margin with 5 pinnate, stout setae (more proximal 2 setae longer than distal ones), 2 simple slender setae; dactylus ventral margin with fringed of fine setae proximally plus 2 bifid stout setae, distal claw 0.55× as long as article, 5 distal setae between claws.

Pereopods II–IV (Fig. 5C–E) inserted on coxae laterally; anteromedian margin of basis protruded sharply, basis of pereopod II, III with 2 broom setae plus simple seta on anterior edge, basis of pereopod IV with 4 broom setae plus simple seta, small seta on distoposterior corner, basis, 1.8× longer than wide; ischium, 2.3× longer than wide, slightly shorter than basis, pereopods II, III with pair of simple setae on both side of

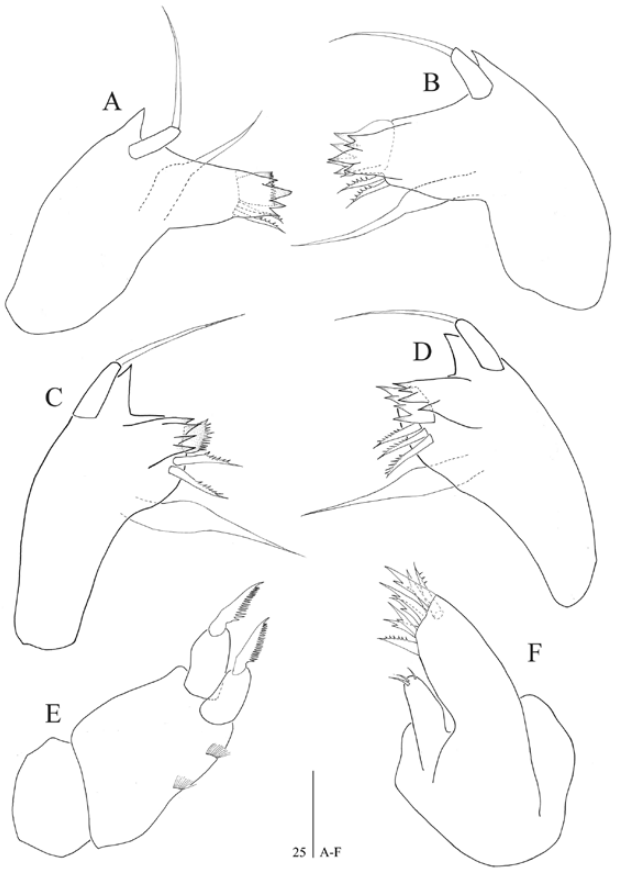

Figure 4. *Coxicerberus fukudai*, male: left mandible, dorsal (**A**); right mandible, dorsal (**B**); left mandible, medial (**C**); right mandible, medial (**D**); maxilla, dorsal (**E**); maxillula, dorsal (**F**). Scale bar: 25 µm, 1000×.

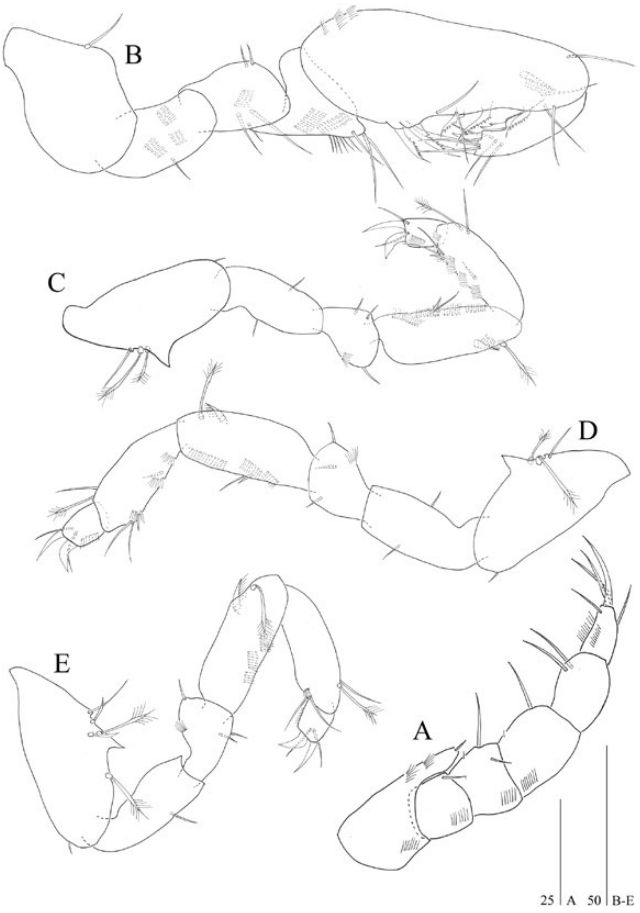

Figure 5. *Coxicerberus fukudai*, male: maxilliped, dorsal (**A**), pereopod I, lateral (**B**); pereopod II, lateral (**C**); pereopod III, lateral (**D**); pereopod IV, lateral (**E**). Scale bars, A–D: 50 µm, E: 25 µm, 1000×.

margin, pereopod IV with one seta on anterior margin; merus 1.1× longer than wide, distinctly shorter than ischium, broaden distally, with spinular row on anterior middle edge, pair of setae on posterior margin, seta on anterior distal corner; carpus of pereopods II, III with 4 spinular, pereopod IV with 3 spinular rows, broom seta, robust pinnate seta on anterodistal margin, simple seta plus short, robust seta on posterior middle margin, carpus, 2.8× longer than wide; propodus approximately as long as carpus 0.9, 2.8× longer than wide, propodus of pereopod II with 4 spinular rows, pereopods III, IV with 3 spinular rows along posterior margin, 2 simple setae anterior distal corner, 2 simple setae on posterior distal corner; dactylus almost rectangular, 1.2× longer than wide, with pair of claws, one slender, one curved on distal end, with spinular row of setae plus 2 setae on ventral margin.

Pereopods V–VII (Fig. 6A–C) with almost same shape as preceding ones; basis with 2 or 3 broom setae plus simple seta on posterior middle margin; ischium with 2 setae on anterior, posterior middle margins except pereopod V with elongated seta on distal margin plus simple seta on anterior middle margin, merus widened distally, with seta on anterior distal corner, spinular row of setae on posterior middle margin; carpus longer than merus, with broom seta on posterior distal corner plus simple seta on distal margin, robust seta on anterior ventral margin plus spinular row near dorsal proximal base; propodus with spinular row of setae plus seta near proximal end, pereopods V, VI with 2 setae on posterior distal corner plus simple seta on anterior distal corner, pereopod VII with 2 pairs of setae; dactylus with simple seta, claws on distal end curved anteriorly.

Labium (Fig. 6D) with incurved lobes, with 2 lobes, more than 6 setae plus fine setules along distal margin.

Pleopod I absent. Male pleopod II (Figs. 7A, 8C–F, 9A–C) with both coxae fused into single rectangular plate; protopod rectangular, 2.8× longer than wide; mediodistal corner of each basis with several spinular rows (see Fig. 8D); exopodite much smaller than endopodite, length 0.26× of endopodite, protruded ventrally, with apical seta (see Fig. 9C); endopodite, outcurved, 2.1× longer than wide, tapering distally, several spinules covering medial margin (see Fig. 8E, F), lateral end of endopodite extended, with 2 triangular spines on medial end of right apical end, triangular spine on left end (see Fig. 9A, B), with long appendix masculina, distinctly separated from endopodite, almost reaching to end of pleotelson.

Pleopod III (Fig. 7B) uniramous; tapering distally, slightly longer than endopodite of pleopod II excluding long appendix masculina; inner margin 5 lobed, each lobe pinnate; simple seta on proximal margin.

Pleopod IV (Fig. 7C) covered by pleopod III; second part bilobed, segmentation indistinct.

Uropods (Figs. 7D, 9D) with globular protopod, as long as wide; 3 spinular rows along medial margin, 2 setae on lateral edge, seta on mediodistal corner, seta on ventrodistal edge; exopodite much smaller than endopodite, with 2 setae; endopodite, 2.6× longer than wide, tapering distally, with 8 setae on distal margin, 2 of which broom-like, 2 elongated setae on distal end.

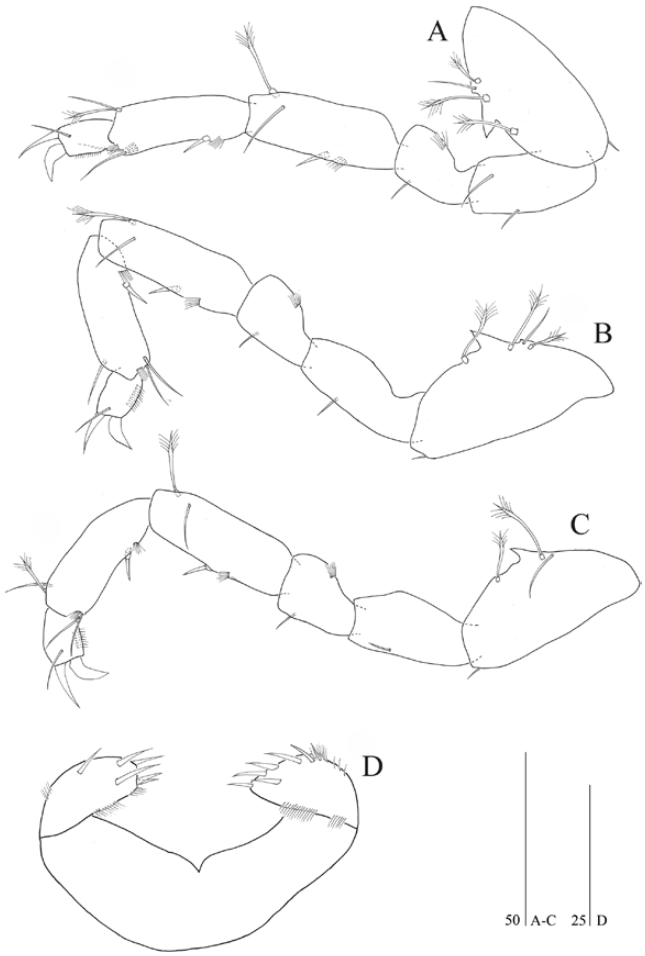

Figure 6. *Coxicerberus fukudai*, male: pereopod V, lateral (**A**); pereopod VI, lateral (**B**); pereopod VII, lateral (**C**); labium, dorsal (**D**). Scale bars, A–C: 50 µm, D: 25 µm, 1000×.

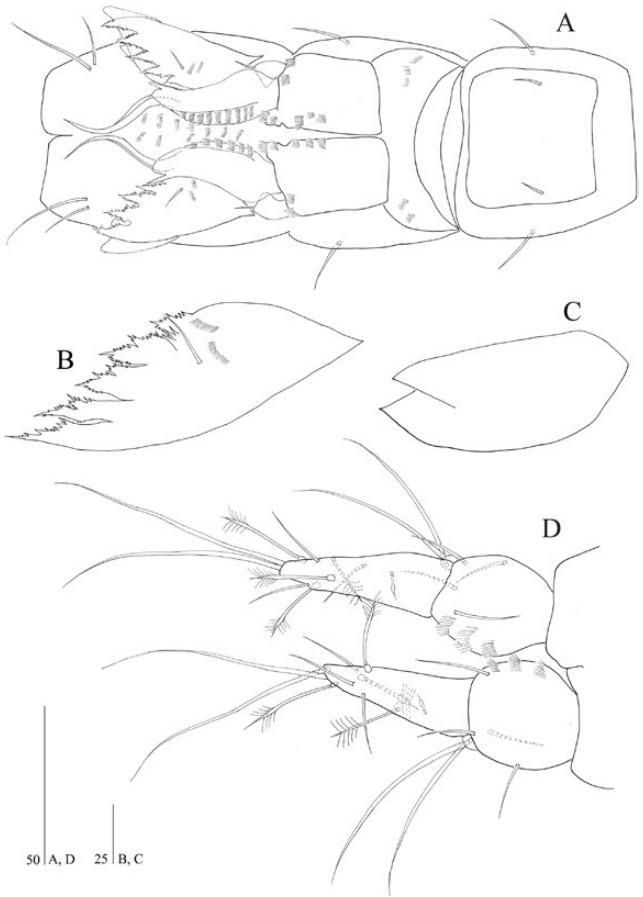

Figure 7. *Coxicerberus fukudai*, male: pleotelson with pleopod II and III, ventral (**A**); pleopod III, dorsal (**B**); pleopod IV, dorsal (**C**); uropods, dorsal (**D**). Scale bars, A, D: 50 µm, B, C: 25 µm, 1000×.

Male penial papillae (Fig. 8B) at ventral margin of pleonite VII, with 2 trapezoidal lobes, one distal groove, respectively.

Phylogeny and haplotype diversity

Partial mtCOI and Cytb sequences were successfully obtained from 27 and 24 specimens, respectively (Supplementary material Table S1). Final alignment included 29 mtCOI sequences, including two outgroups. It was trimmed to the same length, 556 base pairs, of which 371 characters were constant, 185 variables, and 96 parsimony informatives. No stop codons were detected and sequences gave translated polypeptide of approximately 185 amino acids. The final alignment of the Cytb sequences contained 24 sequences, 321 base-pairs long, of which 292 characters were constant, 29 variables, and 27 parsimony informatives. The sequences translated into a polypeptide of approximately 107 amino acids and revealed no stop codon. Tamura-Nei (Tamura & Nei, 1993) with invariable sites (TrN+I), and Transition model (Posada, 2003) (TIM 1) were chosen as the best fit models for both mtCOI and Cytb, respectively. The resulting phylograms from both ML and BI analysis had nearly identical topologies supported by high Bootstrap values and Bayesian posterior probabilities. Hence, only the ML phylogram analysis is presented here (Figs. 10, 11). Two distinctly diverged monophyletic lineages within the in-group taxa were present on the mtCOI phylogram. All Japanese sequences (H1-8) clustered together with the Korean populations (lineage A in Fig. 14), whereas the Byeonggok and Jangsa beaches sequences (Fig. 10, B2, J) from Korea formed another clade (lineage B in Fig. 10). The results of the Cytb analysis also supported the existence of two distinct lineages (Fig. 11). The Jangsa sequences (Ja) formed a distinct clade with Wolpo, Dogu, and Imrang beaches (Fig. 11), whereas the Gazin sequences (Fig. 11G) clustered with the Heunghan (HH) and Japanese populations (H). The results of the K2P distances calculations are shown in Supplementary material Tables S4 and S5. The K2P distances between mtCOI sequences of the ingroup and outgroup taxa ranged between 32% and 38%, whereas distances among the ingroup taxa varied from 0.0% and 10.6%. The distances between Cytb ingroup sequences ranged from 0.0% and 9.5%. This indicates that the divergence rate of mtCOI is relatively faster than that of Cytb in the case of *Coxicerberus*. The mtCOI and Cytb distances within each diverged clade, however, are 0.02% and 0.03%, respectively. Because no significant variations among the examined ribosomal 18S V7 expansion segment sequences were observed, all these sequences were excluded from further analysis.

The haplotype network constructed with 27 mtCOI sequences was 567 base-pairs long, with 56 variable sites, 3 singletons, and 53 parsimony informative sites. The average nucleotide composition was 30.2%, 25%, 25.5%, and 19.3% for each T, C, A, G, respectively, therefore being slightly more AT (55.7%) rich. Nucleotide diversity (π) and haplotype diversities (Hd) for each population is shown in Supplementary material Table S3. A total of seven haplotypes were detected, with Byeonggok (Fig. 12A) having three haplotypes, one of which was very distinct with 52 mutational steps to the other two, and was also present further south at Jangsa beach (Fig. 1J). Byeonggok beach was the only location where two distinct haplotypes were found in sympatry (Figs. 1B, 12A). Differences between other six haplotypes were minimal, with up to five mutational changes (Fig. 12A), all belonging to lineage A (Fig. 10). Lineage A had 0.00072 ± 0.00027 π and 0.367 ± 0.122 Hd, whereas lineage B displayed no significant differences in both nucleotide and haplotype diversity due to the small number of sequences examined. Haplotype network constructed based on the Cytb sequences was identical with the mtCOI network in terms of the haplotype distribution among clades (Fig. 12B). Our analysis was based on 24 sequences, 321 base-pairs long. The sequences were slightly richer in AT (59.8%) pairs. We detected a total of eight haplotypes, with lineage B having more nucleotide diversity (0.00328 ± 0.00109 π), than lineage A (0.00215 ± 0.0005 π), but slightly less haplotype diversity (0.538 ± 0.161 Hd; 0.618 ± 0.104 Hd). Overall, Cytb showed a higher haplotype and nucleotide diversity. Results of the mtCOI analysis were mostly derived from populations belonging to the lineage A (Supplementary material Table S2), and direct comparison of lineages had some limitations since they were unequally represented in the data set. Comparison between lineages using Cytb data was relatively informative, and highlights the differences between the two clades and their haplotype distribution.

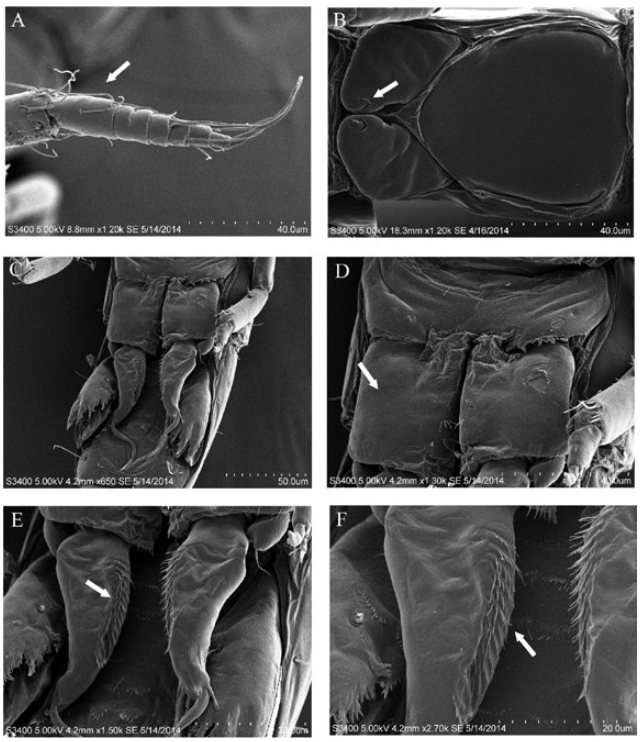

Figure 8. *Coxicerberus fukudai*, male: SEM image; flagellum of antenna (**A**); ventral view of pereonite VII (**B**); ventral view of pleotelson (**C**); basis of pleopod II (**D**); endopodite of pleopod II (**E**); spinular rows of endopodite (**F**).

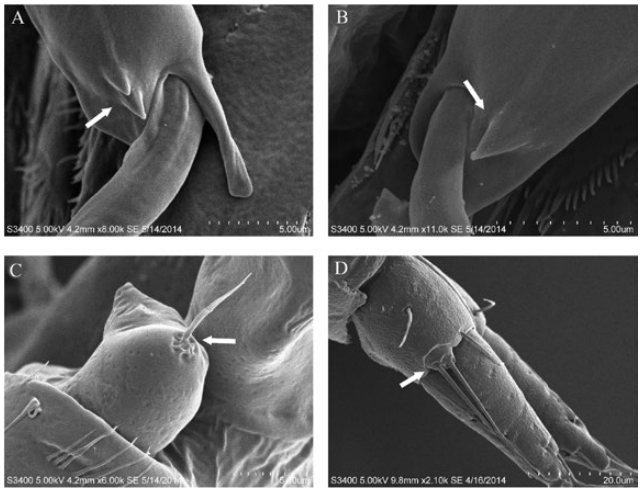

Figure 9. *Coxicerberus fukudai*, male: SEM image; right apical part of endopodite of pleopod II (**A**); left apical part of endopodite of pleopod II (**B**); exopodite of pleopod II (**C**); exopodite of uropods (**D**).

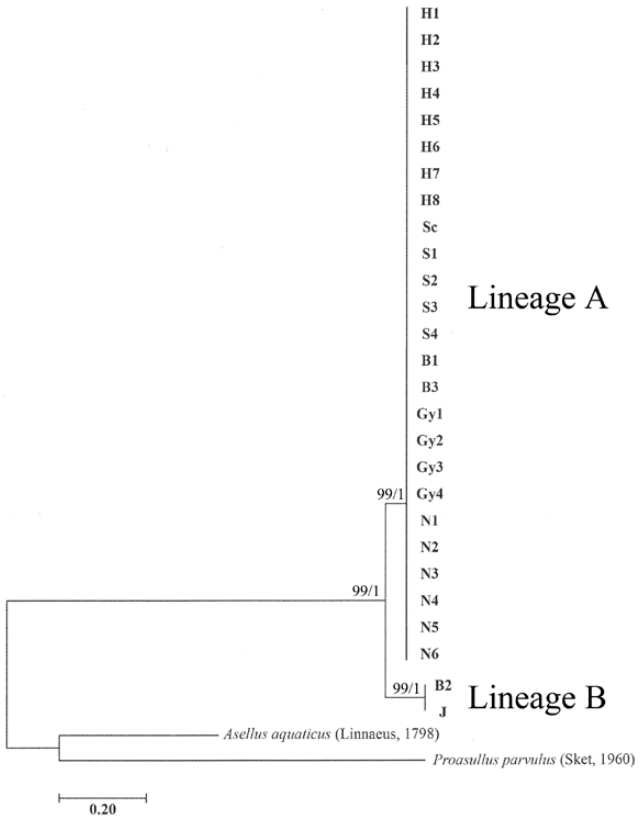

Figure 10. Maximum-likelihood (ML) phylogram of Korean and Japanese populations based on mtCOI sequences. These phylograms was rooted with *Proasellus parvulus* YCD534, and *Asellus aquaticus* FJ749279 clades. Scale shows substitutions per site. Numbers above the branches represent bootstrap support and Bayesian posterior probabilities.

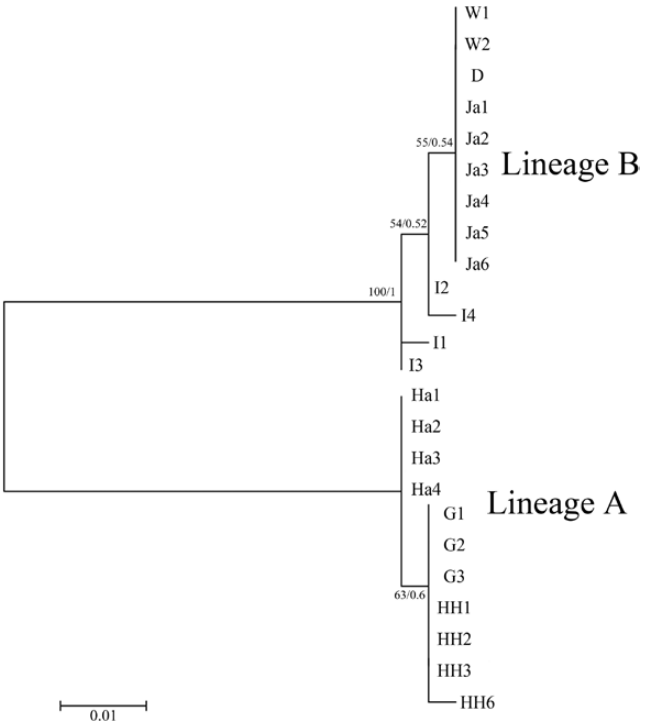

Figure 11. Maximum-likelihood (ML) phylogram of Korean and Japanese populations based on Cytb sequences. These phylograms is unrooted. Scale shows substitutions per site. Numbers above the branches represent bootstrap support and Bayesian posterior probabilities.

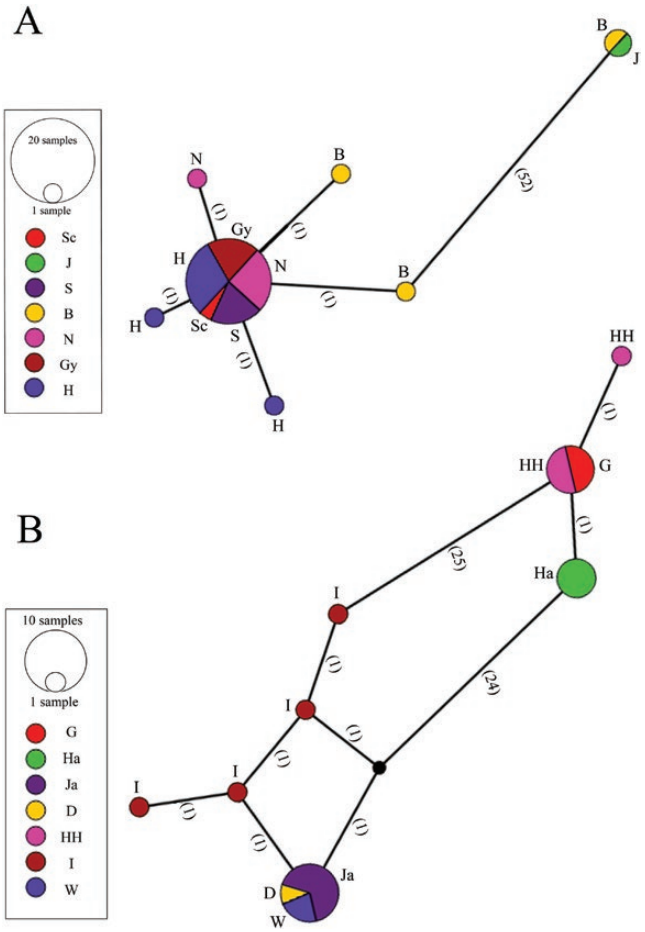

Figure 12. The plausible set of haplotype networks of the mtCOI (**A**); the haplotype networks of Cytb (**B**). Numbers in parenthesis indicate the number of mutations; letters represent the unique haplotype, which are color-coded according to the region. The diameter of the circles is proportional to the number of haplotypes sampled.

Detection of Wolbachia

We amplified only around 200–300 base pairs of the wsp gene region, much less than its anticipated length (575–625bp) when using the primers wsp81F and wsp691R (Braig *et al.*, 1998; Zhou *et al.*, 1998; Shoemaker *et al.*, 2000, 2004; Baudry *et al.*, 2003). BLAST alignment, however, identified *Wolbachia* sequences despite low coverage. Our analysis using 42 specimens of *C. fukadai* isolated from all localities revealed a peculiar geographic distribution of the *Wolbachia* infections. A total of 23 individuals (55%) were detected positive for *Wolbachia*, all from localities between Byeonggok (Fig. 1B) and Imrang beaches (Fig. 1I), whereas no infected individuals from the northern sites between Gazin and Samcheock beaches in Korea, and Hamakoshimizu in Japan, were found (Fig. 1G–S, Supplementary material Table S3). With the exception of Heunghan beach, where six individuals were identified as belonging to lineage A (Supplementary material Table S3), all the other infected individuals belonged to lineage B.

Morphological analysis

All specimens studied were identified as *C. fukudai* based on the following characters: 1) antennula with six articles; 2) antenna with six-segmented flagellum; 3) outer lobe of maxillula with eight robust setae on the distal margin and inner lobe with three short apical setae; 4) male penial papillae with two trapezoidal lobes containing distomedial grooves on the ventral surface of

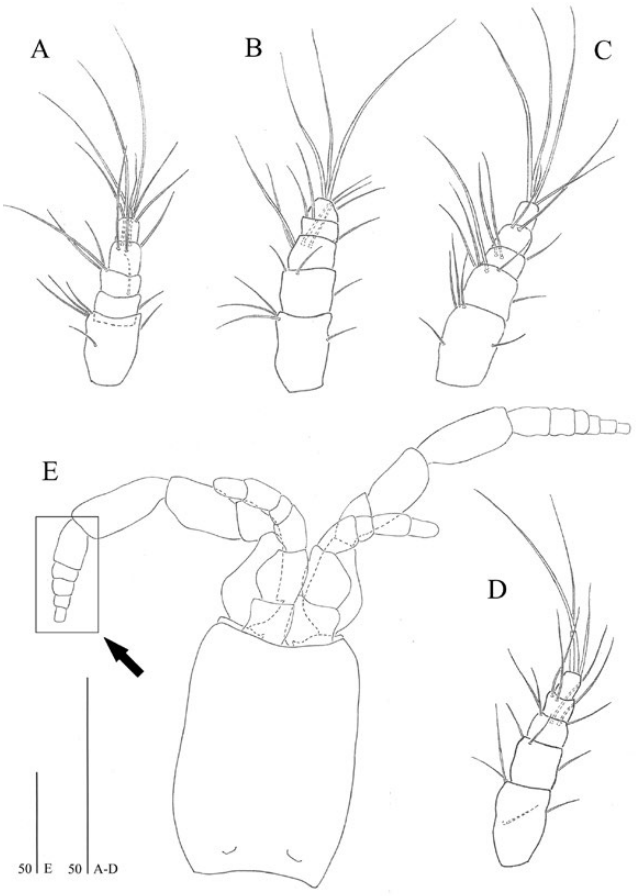

Figure 13. Morphological abnormalities of the antennal flagellum of *Coxicerberus fukudai*, Male, Jangsa slide no. 20 (**A**); male, Jangsa slide no. 13 (**B**); male, Jangsa slide no. 15 (**C**); male, Jangsa slide no. 11 (**D**). Dorsal view of the cephalon. The black square indicates and abnormal flagellum with five segments, Jangsa slide no. 11 (**E**). Scale bar: 50 µm, 1000×.

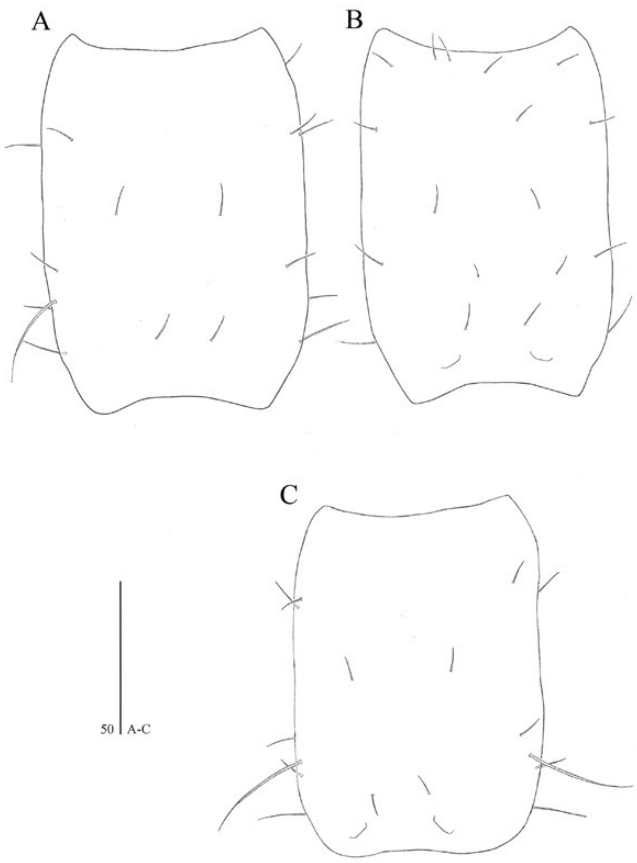

Figure 14. Morphological abnormalities of the dorsal setal position of the cephalon of *Coxicerberus fukudai*. Male, Jangsa slide no. 8 (**A**); male, Jangsa slide no. 4 (**B**); male, Jangsa slide no. 5 (**C**). Scale bar: 50 µm, 1000×.

pereonite 5; 5) male endopods of pleopod II distally tapered, showing incurved lateral margin, several spinular rows on medial margin, and long, twisted appendix masculina; and 6) females with ventral semicircular extrusions on pereonite V. We also noted several morphological characters of the Korean male specimens that differ from the original description (Ito, 1974). We examined the syntype of *C. fukudai*, but could not find any significant differences because of the incomplete nature of the syntype specimen. Comparison between the original description and the males from Sokcho, Korea showed the following differences: 1) one of the three setae on the antennular article I of the Korean specimens are broom-like seta, but those in the original description are given as consisting of three simple setae; 2) the antennular article II in the Korean specimen has one simple and one broom-like seta distomedially, but two simple setae in the description; 3) the antennular article IV of Korean specimens has two broom-like setae, one longer than the other, but the two setae are of a similar size, one of them smooth, in the description; 4) article I of the antennal flagellum in the Korean specimens is longer than wide (L:W ratio 1.58), but it has a ratio of 1.03 according to the drawings of Ito (1974); 5) the antennal article VI in the original description has ten setae, thirteen setae in the Korean specimens; 6) the maxillipedal palp articles II and III of the Korean specimens have one and two setae, respectively, one seta on article III, which is situated anteromedially, in the original description; 7) the original description and the Korean specimens also have different chaetotaxy of the pereopods (Table 1); and 8) whereas the uropodal exopodite in the Korean specimen is armed with ten setae distally (five of them broom-like), but there are nine and eight setae, respectively, according to the description. No morphological differences between Korean and Japanese females were detected with the exception of the body size (1.13 *versus* 1.05 mm).

In addition to the differences between the original description and our specimens, we also detected an unusual abnormality in the morphology of the antennal flagellum among the individuals of lineage B. The antennal flagellum of *Coxicerberus* typically has five to seven articles, and fully matured as well as juveniles of *C. fukudai* have a six-segmented antennal flagellum (Fig. 2C). Some of the specimens from Byeonggok and Jangsa beaches (2 of the 20 males from Byeonggok and 3 of the 20 males from Jangsa) had an asymmetrical number of antennal flagella. One side of the antenna had a five-segmented flagellum in contrast to the opposite one (Fig. 13E). The following characters underline the morphological abnormality of the five-segmented flagellum: 1) the L:W ratio of article I was identical to the six-segmented one, but one of the abnormal specimens had four instead of five setae (Fig. 13B, D); 2) one of the abnormal specimens had three setae on the distal corner of article II, whereas the normal one had one seta at the same site (Fig. 13C); and 3) the chaetotaxy of article III of the abnormal flagellum was identical to the normal one, but article IV was identical to article V of the normal flagellum and article V was identical to article VI of the normal flagellum (Fig. 13). It seems that the asymmetrical forms lost the article corresponding to the fourth article of the normal flagellum. Asymmetrical forms were only apparent on the dorsal view of the left antenna. Other abnormalities were also observed in the cephalon, such as more setae on the dorsal surface than in the normal form (Fig. 14).

Table 1. Comparison of the pereopods armature formula between Korean specimens of *C. fukudai* and the original description in Ito (1974). Numbers indicate the number of simple setae; [ ], numbers of broom setae; ( ), numbers of short setae.

	Basis	Ischium	Merus	Carpus	Propodus	Dactylus
Korean specimens						
Pereopod II	1,[2],(1)	2	3	1,[1],(2)	3,[1],(2)	2
Pereopod III	1,[2],(1)	2	3	1,[1],(2)	3,[1],(2)	2
Pereopod IV	1,[4],(1)	1	3	[2],(1)	3,[1]	2
Pereopod V	1,[3],(1)	2	1	1,[1],(1)	3,[1],(1)	1
Pereopod VI	1,[3],(1)	1	1	1,[1],(1)	3,[1],(1)	1
Pereopod VII	1,[2],(1)	1	1	1,[1],(1)	3,[1],(1)	1
Original description						
Pereopod II	1,[2],(1)	2	2	1,(1)	3,[1],(1)	2
Pereopod III	1,[2],(1)	2	2	1,[1],(1)	3,[1],(1)	2
Pereopod IV	1,[2],(1)	2	2	1,[1],(1)	3,[1],(1)	2
Pereopod V	1,[2],(1)	2	2	2,(1)	3,[1],(1)	1
Pereopod VI	1,[2],(1)	2	2	2,(1)	3,[1],(1)	1
Pereopod VII	1,[2],(1)	2	2	[1],(1)	3,[1],(1)	1

There were no further morphological differences between the normal individuals of the two lineages, and the size range was also similar in males (0.7–0.9 mm) and females (0.9–1.2 mm).

DISCUSSION

Two diverged lineages in the Korean populations

Development of the molecular tools in the past several decades has aided tremendously in biodiversity and phylogenetic studies (Pfenninger & Schwenk, 2007; Bradford *et al.*, 2010), and has considerably increased the number of cryptic species worldwide, being evenly distributed among major metazoan taxa and biogeographic regions (Hebert *et al.*, 2004; Bickford *et al.*, 2007; Karanovic *et al.*, 2016). Several studies have shown that the degree of molecular differentiation associated with cryptic species among isopods varies among groups (Held & Wägele 2005; Raupach *et al.*, 2007, 2014; Markow & Pfeiler, 2010; Varela & Haye, 2012; Yin *et al.*, 2013; Brix *et al.*, 2014; Lee *et al.*, 2014; Hurtado *et al.*, 2017).

Results of our molecular analysis uncovered diverged lineages within the Korean populations of *C. fukudai*. Sequences belonging to lineages A and B differed by over 11% in the K2P distances, whereas the intraclade distances ranged between 0.0%–2% (Supplementary material Table S4). These values agree well within intra/interspecific variation proposed by previous isopod studies. The pattern of the Cytb was similar to mtCOI (Supplementary material Table S5). Although the criterion for the species delimitation based on this marker is not so well understood as in mtCOI (Lefébure *et al.*, 2006; Costa *et al.*, 2007; Matzen da Silva *et al.*, 2011), most of the Cytb sequences from Jangsa to Imrang beaches form a distinct lineage from the rest of the Korean and Japanese populations (Fig. 11). The haplotype network analysis showed an obvious geographical distributional pattern, with haplotypes of the lineage B being dominant in the southern regions, whereas those of the lineage A were dominant in the northern region (Fig. 12). Byeonggok beach seems to be the intersection where the distinct haplotypes are found in sympatry (Fig. 12A). The presence of cryptic species in the Korean populations is apparent, given the lack of differences in the morphology between the two clades.

High intraspecific molecular divergence rates and low morphological variability detected in the Korean populations are the first such case among microcerberidean isopods. It raises another question on the multiple occurrences of cryptic species in morphologically homogenous groups such as Microcerberidae. Given the generally accepted mutation rates of mtCOI in crustaceans in the range of 1.5% to 2.6% per millions of years (Knowlton & Weigt, 1998), the two Korean lineages might have separated from their most recent common ancestor between 3.6 and 2.1 mya. Since they have been found together only in one locality, their sympatry may be explained by the subsequent colonization events. A very low divergence rates between Korean and Japanese populations belonging to the lineage A (Supplementary material Tables S4, S5) indicates that the two populations separated very recently. Eurasia and Japan were connected through the Soya land bridge between Sakhalin and Hokkaido, and the Tsushima and Korean land bridges between Korea and Kyushu island from the Middle until the Late Pleistocene (Dobson, 1994; Millien-Parra & Jaeger, 1999). The dispersal of lineage A (northeastern part of Korea and Hamkoshimizu) probably took place via the Soya land bridge connecting Japan and Sakhalin. This may have been the last communication between the populations. Some exceptional cases of minute crustaceans crossing large scale geographical barriers have nevertheless been recorded. Menzel *et al.* (2011) listed 61 species of *Mescletodes* Sars, 1909 (a group of sediment-dwelling harpacticoid copepods) collected from a wide area: North Atlantic, central Pacific, southern Indian Ocean, Southern Ocean, and the Mediterranean Sea. Easton & Thistle (2016) discovered that some of the deep-sea harpacticoids could have a distribution scale of over 1000 km despite their limited dispersal ability. Some species of the deep-sea isopod *Macrostylis* Sars, 1864 show remarkable distributional and depth ranges near Amundsen Sea in Antarctica (Riehl & Kaiser, 2012). These authors proposed that, instead of individual motility, bottom current and other erosion deposition events were much more important factors contributing to such a wide area of distribution. In the case of *Coxicerberus*, however, studies on the dispersal abilities and survivorship at diverse depth ranges are lacking. Most of the known species were found from marine shallow interstitial or subterranean waters around the world. The Korea Marine Environment Management Corporation (2014) had no record of microcerberid isopods among the collected crustaceans, despite using suitable equipment for meiofauna collection. Although there are cases of large scale distribution of minute crustaceans with weak mobility in deep-sea, it is difficult to directly compare them with micrcerberids that live in different environments. The hypothesis that the dispersal of *C. fukudai* between Korea and Japan occurred via a land bridge is thus more probable than via open ocean. Ito (1974) found a strong morphological similarity between *C. abbotti* and *C. fukudai*, the former being reported along the North American Pacific coast (Lang 1961). It appears that the microcerberids can achieve a wide distribution without major morphological changes.

Factors that might have influenced haplotype diversity

The evolution of mitochondrial DNA can be influenced not only by geographical processes but also by factors such as introgressive hybridization, incomplete lineage sorting, and heteroplasmy, all possibly leading to the misinterpretation of the organism's evolutionary history (Barber *et al.*, 2012). With respect to heteroplasmy, several previous studies observed atypical mtDNA genome structure in diverse groups of isopods, especially in the terrestrial ones such as *Armadillidium vulgare* (Latreille, 1804) and *Porcellio pruinosus* Arcangeli, 1935. Both species have a genome structure with "head to head" dimers and linear monomers (about 14 kb), transmitted maternally, which possibly correlate with the presence of heteroplasmy, and is leading to the changes in phenotype such as dual expression of tRNA alanine/valine (Raimond *et al.*, 1999; Marcadé *et al.*, 2007; Doublet *et al.*, 2012). In other aquatic isopods, Doubl *et al.* (2012) observed atypical mtDNA in *Asellus aquaticus* (Linnaeus, 1758), and due to the basal position of Asellota in the phylogeny of isopods, the authors assumed an early appearance of the atypical mtDNA in the evolutionary history of isopods. There is nevertheless no evidence of the atypical mtDNA genome structure in the suborder Microcerebridea. According to Brusca & Wilson (1991), Microcerberidea is assumed to be closely related to Asellota, and future studies of genome structure may shed the light on the possible correlation between genome structure and phylogenetic position.

Maternally inherited microbes, such as *Wolbachia*, can also affect the mtDNA evolution of the host (Hurst & Jiggins, 2005). This has been largely supported by several studies examining the several groups of arthropods (Marcadé *et al.*, 1999; Shoemaker *et al.*, 1999, 2003, 2004; Baudry *et al.*, 2003; Dean *et al.*, 2003; Jiggins, 2003; Narita *et al.*, 2006). Among crustaceans, terrestrial isopods are well known for a high rate of *Wolbachia* infection (Bouchon *et al.*, 1998; Rigaud *et al.*, 1999; Stouthamer *et al.*, 1999; Cordaux *et al.*, 2001, 2012; Moret *et al.*, 2001; Le Clec'h *et al.*, 2013). A few studies on the correlation between the infection and mtDNA variations have been carried out (Grandjean *et al.*, 1993; Marcadé *et al.*, 1999; Raupach *et al.*, 2014). These revealed a negative effect of *Wolbachia* infection on the host, causing cytoplasmic incompatibility (mating between infected and uninfected parents results in a high level of embryonic mortality and male killing). Infection can influence mitochondrial DNA diversity, including the number of segregation sites, nucleotide diversity, and haplotype diversity (Shoemaker *et al.*, 2004). Our screening for the presence of *Wolbachia* in the populations of *C. fukadai* showed a high infection rate in the B-lineage populations, whereas the lineage-A populations were much less affected, with *Wolbachia* detected in only one locality (Supplementary material Table S3). Our results also showed that infected populations had higher haplotype diversity. This observation is not well matched to those of previous studies on the effects of *Wolbachia* infections, since they indicate a decrease in haplotype and nucleotide diversities in infected populations (Dean *et al.*, 2003; Shoemaker *et al.*, 2004; Hurst & Jiggins, 2005; Gerth *et al.*, 2011). All the southern populations from Byeonggok beach (either belonging to lineage A or B) were infected, whereas all other northern populations (only lineage A) were not (Fig. 1, Supplementary material Table S3). It also remains unclear whether temporal sampling at different localities and seasons could possibly cause infection rate directly, a problem already addressed in Raupach *et al.* (2014).

Morphological variability of C. fukudai

Although we failed to recognize meaningful differences in the syntypes (25-VII-73, 9-VIII-67a) due to their poor preservation, several morphological differences were observed between the males of Korean *C. fukudai* and the original description (Ito, 1974). The differences were mostly related to the chaetotaxy of appendages and the L:W ratio of the antennal flagellum. Such differences in chaetotaxy sometimes can occur via allometric development and damage caused by sampling or dissecting. Ito (1974) mentioned that his description of the endopod of the male pleopod II was not certain due to the magnification limit of his microscope. If this is true, the morphological difference we have found may be the result of Ito's misinterpretation of the character. It is thus hard to tell whether these represent intraspecific variability in *C. fukudai* or are indication of morphospecies until the type material is thoroughly examined. No significant morphological differences were found in females, but female morphological characters are often not enough for delineation of isopod species and several similar cases have been reported in other groups, Haploniscidae and Macrostylidae (Brökeland, 2010; Riehl & Brandt, 2010). The Japanese locality from where our samples were collected is the type locality of *C. fukudai*, Hamakoshimizu, Hokkaido. Ito (1974) stated that many specimens were also collected from Tombetsu beach on Hokkaido (about 212 km north from Hamakoshimizu), but he did not provide any comments on the possible morphological differences between the males of the two populations. There are several cases of microcerbrids (*M. abbotti*, *M. remanei*, and *M. anfindicus*) having a wide distribution and a very subtle intraspecific variation (Baldari & Argano, 1984). Since we already found potentially cryptic and sympatric species in Korea, it is possible that Hamakoshimizu beach hosts true *C. fukadai* and another species, which we collected and found also in parts of Korea.

We found morphological abnormalities in several specimens of lineage B. But since the abnormalities were not detected in all specimens of lineage B, they could be considered part of the phenotypic plasticity. Similar asymmetric variation was also reported from a single specimen of *M. anfindicus*, showing a curious abnormality in segmentation of the endopodite of the male pleopod II, which resembles that of the pereopod (Baldari & Argano, 1984). Application of more sensitive methods for detecting morphological differences, such as geometric morphometrics (Klingenberg *et al.*, 2000, 2003; Karanovic *et al.*, 2016) could aid detection of different morphological species in the *C. fukadai* complex.

SUPPLEMENTARY MATERIAL

Supplementary material is available at *Journal of Crustacean Biology* online.

S1 Table. Specimens used in the molecular analysis.
S2 Table. Results of DNA diversity analysis.
S3 Table. Comparison of *Wolbachia* infection rates.
S4 Table. K2P distances of mtCOI among the sequences.
S5 Table. K2P distances of Cytb among the sequences.

ACKNOWLEDGEMENTS

We are grateful to S.F. Hiruta (Hokkaido University) for collecting the material from type locality of *C. fukudai* in Japan. Thanks to S. Kim and R. Jeong (Hanyang University, Korea) for sampling and useful comments on the research. We also thank two anonymous reviewers for their kind and helpful comments. This study was supported by the BK21 Plus Program (Eco-Bio Fusion Research Team, 22A20130012352) funded by the Ministry of Education (MOE, Korea). This study was also supported by grant NIBR201601201 from the National Research Foundation of Korea (NRF) and National Institute of Biological Resource (NIBR) funded by the Ministry of Environment (MOE), Republic of Korea.

REFERENCES

Akaike, H. 1974. A new look at the statistical model identification. *IEEE Transactions on Automatic Control*, **19**: 716–723.

Albuquerque, E.F., Meurer, B. & Netto, G.D.C.G. 2009. Effects of temperature and salinity on the survival rates of *Coxicerberus ramosae* (Albuquerque, 1978), an interstitial isopod of a sandy beach on the coast of Brazil. *Brazilian Archives of Biology and Technology*, **52**: 1179–1187.

Altschul, S.F., Gish, W., Miller, W., Myers, E.W. & Lipman, D.J. 1990. Basic local alignment search tool. *Journal of Molecular Biology*, **215**: 403–410.

Arcangeli, A. 1935. Isopodi terrestri di caverne della Spagna (collezione del Museo di Storia Naturale di Madrid). *Eos*, **10**: 171–195.

Baldari, F. & Argano, R. 1984. Description of a new species of *Microcerberus* from the South China Sea and a proposal for a revised classification of the Microcerberoidea (Isopoda). *Crustaceana*, **46**: 113–126.

Barber, B.R., Xu, J., Pérez-Losada, M., Jara, C.G. & Crandall, K.A. 2012. Conflicting evolutionary patterns due to mitochondrial introgression and multilocus phylogeography of the Patagonian freshwater crab *Aegla neuquensis*. *PLoS ONE*, **7**: e37105.

Baudry, E., Bartos, J., Emerson, K., Whitworth, T. & Werren, J.H. 2003. *Wolbachia* and genetic variability in the birdnest blowfly *Protocalliphora sialia*. *Molecular Ecology*, **12**: 1843–1854.

Bickford, D., Lohman, D.J., Sodhi, N.S., Ng, P.K., Meier, R., Winker, K., Ingram, K.K. & Das, I. 2007. Cryptic species as a window on diversity and conservation. *Trends in Ecology & Evolution*, **22**: 148–155.

Bouchon, D., Rigaud, T. & Juchault, P. 1998. Evidence for widespread *Wolbachia* infection in isopod crustaceans: molecular identification and host feminization. *Proceedings of the Royal Society of London, B: Biological Sciences*, **265**: 1081–1090.

Boyko, C.B., Bruce, N.L., Hadfield, K.A., Merrin, K.L., Ota, Y., Poore, G.C.B., Taiti, S., Schotte, M. & Wilson, G.D.F. (eds.) (2008 onwards). *World marine, freshwater and terrestrial isopod crustaceans database* [http://www.marinespecies.org/isopoda/].

Bradford, T., Adams, M., Humphreys, W.F., Austin, A.D. & Cooper, S.J.B. 2010. DNA barcoding of stygofauna uncovers cryptic amphipod diversity in a calcrete aquifer in Western Australia's arid zone. *Molecular Ecology Resources*, **10**: 41–50.

Braig, H.R., Zhou, W., Dobson, S.L. & O'Neill, S.L. 1998. Cloning and characterization of a gene encoding the major surface protein of the bacterial endosymbiont *Wolbachia pipientis*. *Journal of Bacteriology*, **180**: 2373–2378.

Brix, S., Svavarsson, J. & Leese, F. 2014. A multi-gene analysis reveals multiple highly divergent lineages of the isopod *Chelator insignis* (Hansen, 1916) south of Iceland. *Polish Polar Research*, **35**: 225–242.

Brökeland, W., 2010. Description of four new species from the *Haploniscus unicornis* Menzies, 1956 complex (Isopoda: Asellota: Haploniscidae). *Zootaxa*, **2536**: 1–35.

Brusca, R.C. & Wilson, G.D.F. 1991. A phylogenetic analysis of isopoda with some classificatory recommendations. *Memoirs of the Queensland Museum*, **31**: 143–204.

Chappuis, P.A. 1942. Eine neue Methode zur Untersuchung der Grundwasserfauna. *Acta Scientifica Mathematisch-Naturwissenschaftlichen Universität Francisco-Josephinae, Koloszvar*, **107**: 1–7.

Chappuis, P.A. & Delamare-Deboutteville, C.D. 1954. Recherches sur les crustacés souterrains 103. *Archives de Zoologie expérimentale et générale*, **91**: 103.

Chappuis, P.A. & Delamare-Deboutteville, C.D. 1956. Études sur la fauna interstitielle des îles Bahamas récoltée par Madame Renaud-Debyser. 1. Copepodes et Isopodes. *Vie et Milieu*, **7**: 375–396.

Clement, M., Posada, D. & Crandall, K.A. 2000. TCS: a computer program to estimate gene genealogies. *Molecular Ecology*, **9**: 1657–1659.

Cordaux, R., Michel-Salzat, A. & Bouchon, D. 2001. *Wolbachia* infection in crustaceans: novel hosts and potential routes for horizontal transmission. *Journal of Evolutionary Biology*, **14**: 237–243.

Cordaux, R., Pichon, S., Hatira, H.B.A., Doublet, V., Grève, P., Marcadé, I., Braquart-Varnier, C., Souty-Grosset, C., Charfi-Cheikhrouha, F. & Bouchon, D. 2012. Widespread *Wolbachia* infection in terrestrial isopods and other crustaceans. *Zookeys*, **176**: 123–131.

Costa, F.O., deWaard, J.R., Bouthillier, J., Ratnasingham, S., Dooh, R.T., Hajibabaei, M. & Hebert, P.D.N. 2007. Biological identification through DNA barcodes: the case of the Crustacea. *Canadian Journal of Fisheries and Aquatic Sciences*, **64**: 272–295.

Darriba, D., Taboada, G.L., Doallo, R. & Posada, D. 2012. jModelTest 2: more models, new heuristics and parallel computing. *Nature Methods*, **9**: 772.

Dean, M.D., Ballard, K.J., Glass, A., William, J. & Ballard, O. 2003. Influence of two *Wolbachia* strains on population structure of East African *Drosophila simulans*. *Genetics*, **165**: 1959–1969.

Dobson, M. 1994. Patterns of distribution in Japanese land mammals. *Mammal Review*, **24**: 91–111.

Doublet, V., Raimond, R., Grandjean, F., Lafitte, A., Souty-Grosset, C. & Marcadé, I. 2012. Widespread atypical mitochondrial DNA structure in isopods (Crustacea, Peracarida) related to a constitutive heteroplasmy in terrestrial species. *Genome*, **55**: 234–244.

Easton, E.E. & Thistle, D. 2016. Do some deep sea, sediment dwelling species of harpacticoid copepods have 1000 km scale range sizes? *Molecular Ecology*, **25**: 4301–4318.

Fabricius, J. C., 1798. *Supplementum Entomologiae Systematicae*. Proft & Storch, Hafniae [= Copenhagen].

Felsenstein, J. 1985. Confidence limits on phylogenies: an approach using the bootstrap. *Evolution*, **38**: 16–24.

Folmer, O., Hoeh, W.R., Black, M.B. & Vrijenhoek, R.C. 1994. Conserved primers for PCR amplification of mitochondrial DNA from different invertebrate phyla. *Molecular Marine Biology and Biotechnology*, **3**: 294–299.

Gerth, M., Geißler, A. & Bleidorn, C. 2011. *Wolbachia* infections in bees (Anthophila) and possible implications for DNA barcoding. *Systematics and Biodiversity*, **9**: 319–327.

Goodsir, H.D.S. 1841. On two new species of *Leachia*. *Edinburgh New Philosophical Journal*, **30**: 309–313.

Grandjean, F., Rigaud, T., Raimond, R., Juchault, P. & Souty-Grosset, C. 1993. Mitochondrial DNA polymorphism and feminizing sex factors dynamics in a natural population of *Armadillidium vulgare* (Crustacea, Isopoda). *Genetica*, **92**: 55–60.

Guindon, S. & Gascuel, O. 2003. A simple, fast and accurate method to estimate large phylogenies by maximum-likelihood. *Systematic Biology*, **52**: 696–704.

Hansen, H. J. 1916. Crustacea Malacostraca 3. *Danish Ingolf Expedition 3*, **5**: 1–262

Hebert, P.D.N., Penton, E.H., Burns, J.M., Jansen, D.H. & Hallwachs, W. 2004. Ten species in one: DNA barcoding reveals cryptic species in the neotropical skipper butterfly *Astraptes fulgerator*. *Proceedings of the National Academy of Sciences of the United States of America*, **101**: 14812–14817.

Held, C. & Wägele, J.W. 2005. Cryptic speciation in the giant Antarctic isopod *Glyptonotus antarcticus* (Isopoda: Valvifera: Chaetiliidae). *Scientia Marina*, **69**: 175–181.

Huelsenbeck, J.P., Ronquist, F., Nielsen, R. & Bollback, J.P. 2001. Bayesian inference of phylogeny and its impact on evolutionary biology. *Science*, **294**: 2310–2314.

Hurst, G.D. & Jiggins, F.M. 2005. Problems with mitochondrial DNA as a marker in population, phylogeographic and phylogenetic studies: the effects of inherited symbionts. *Proceedings of the Royal Society of London, B: Biological Sciences*, **272**: 1525–1534.

Hurtado, L.A., Mateos, M. & Liu, S. 2017. Phylogeographic patterns of a lower intertidal isopod in the Gulf of California and the Caribbean and comparison with other intertidal isopods. *Ecology and Evolution*, **7**: 346–357.

Hurvitch, C.M. & Tsai, C.L. 1989. Regression and time series model selection in small samples. *Biometrika*, **76**: 297–307.

Ito, T. 1974. A new species of marine interstitial isopod of the genus *Microcerberus* from Hokkaido. *Journal of the Science Hokkaido University, Series VI. Zoology*, **19**: 338–348.

Ito, T. 1975. A new species of marine interstitial isopod of the genus *Microcerberus* from the Bonin Island. *Annotationes Zoologicae Japonenses*, **48**: 119–128.

Jiggins, F.M. 2003. Male-killing *Wolbachia* and mitochondrial DNA: selective sweeps, hybrid introgression and parasite population dynamics. *Genetics*, **164**: 5–12.

Karaman, S. 1933. *Microcerberus stygius*, der dritte Isopod aus dem Grundwasser von Skoplje, Jugoslavien. *Zoologischer Anzeiger*, **102**: 165–169.

Karanovic, T., Djurakic, M. & Eberhard, S.M. 2016. Cryptic species or inadequate taxonomy? Implementation of 2D geometric morphometrics based on integumental organs as landmarks for delimitation and description of copepod taxa. *Systematic Biology*, **65**: 304–327.

Khalaji-Pirbalouty, V. & Raupach, M.J. 2014. A new species of *Cymodoce* Leach, 1814 (Crustacea: Isopoda: Sphaeromatidae) based on morphological and molecular data, with a key to the Northern Indian Ocean species. *Zootaxa*, **3826**: 230–254.

Kimura, M. 1980. A simple method for estimating evolutionary rate of base substitutions through comparative studies of nucleotide sequences. *Journal of Molecular Evolution*, **16**: 111–120.

Klingenberg, C.P., Barluenga, M. & Meyer, A. 2003. Body shape variation in cichlid fishes of the *Amphilophus citrinellus* species complex. *Biological Journal of the Linnean Society*, **80**: 397–408.

Klingenberg, C.P., Spence, J.R. & Mirth, C.K. 2000. Introgressive hybridization between two species of waterstriders (Hemiptera: Gerridae: *Limnoporus*): geographical structure and temporal change of a hybrid zone. *Journal of Evolutionary Biology*, **13**: 756–765.

Knowlton, N. & Weigt, L.A. 1998. New dates and new rates for divergence across the Isthmus of Panama. *Proceedings of the Royal Society of London, B: Biological Sciences*, **265**: 2257–2263.

Korea Marine Environment Management Corporation. 2014. *National investigation of marine ecosystem, North-East region*. Ministry of Oceans and Fisheries, Seoul, Korea.

Kumar, S., Stecher, G. & Tamura, K. 2016. MEGA7: Molecular Evolutionary Genetics Analysis version 7.0 for bigger datasets. *Molecular Biology and Evolution*, **33**: 1870–1874.

Lang, K. 1961. Contributions to the knowledge of the genus *Microcerberus* Karaman (Crustacea, Isopoda) with a description of a new species from the central California coast. *Arkiv för Zoologi*, **13**: 493–510.

Latreille, P.A. 1804. *Histoire naturelle, générale et particulière des Crustacés et des Insectes.*, **Vol. 14**. F. Dufart, Paris.

Leach, W.E. 1814. Crustaceology. *Brewster's Edinburgh Encyclopedia E. Routledge London*, **7**: 383–384.

Le Clec'h, W., Chevalier, F.D., Genty, L., Bertaux, J., Bouchon, D. & Sicard, M. 2013. Cannibalism and predation as paths for horizontal passage of *Wolbachia* between terrestrial isopods. *PLoS ONE*, **8**: e60232.

Lee, T.R.C., Ho, S.Y.W., Wilson, G.D.F. & Lo, N. 2014. Phylogeography and diversity of the terrestrial isopod *Spherillo grossus* (Oniscidea: Armadillidae) on the Australian East Coast. *Zoological Journal of the Linnean Society*, **170**: 297–309.

Lefébure, T., Douady, C.J., Gouy, M. & Gilbert, J. 2006. Relationship between morphological taxonomy and molecular divergence within Crustacea: Proposal of a molecular threshold to help species delimitation. *Molecular Phylogenetics and Evolution*, **40**: 435–447.

Leigh, J.W. & Bryant, D. 2015. popart: full-feature software for haplotype network construction. *Methods in Ecology and Evolution*, **6**: 1110–1116.

Librado, P. & Rozas, J. 2009. DnaSP v5: a software for comprehensive analysis of DNA polymorphism data. *Bioinformatics*, **25**: 1451–1452.

Linnaeus, C. 1758. *Systema Naturae per Regna Tria Naturae, Secundum Classes, Ordines,Genera, Species, cum Characteribus, Differentiis, Synonymis, Locis.* **Vol. 1**, Edn. 10, Reformata. Laurentii Salvii, Holmiae [= Stockholm].

Marcadé, I., Cordaux, R., Doublet, V., Debenest, C., Bouchon, D. & Raimond, R. 2007. Structure and evolution of the atypical mitochondrial genome of *Armadillidium vulgare* (Isopoda, Crustacea). *Journal of Molecular Evolution*, **65**: 651–659.

Marcadé, I., Souty-Grosset, C., Bouchon, D., Rigaud, T. & Raimond, R. 1999. Mitochondrial DNA variability and *Wolbachia* infection in two sibling woodlice species. *Heredity*, **83**: 71–78.

Markow, T.A. & Pfeiler, E. 2010. Mitochondrial DNA evidence for deep genetic divergences in allopatric populations of the rocky intertidal isopod *Ligia occidentalis* from the eastern Pacific. *Molecular Phylogenetics and Evolution*, **56**: 468–473.

Matzen da Silva, J., Creer, S., Dos Santos, A., Costa, A.C., Cunha, M.R., Costa, F.O. & Carvalho, G.R. 2011. Systematics and evolutionary insights derived from mtDNA COI barcode diversity in the Decapoda (Crustacea: Malacostraca). *PLoS ONE*, **6**: e19449.

Menzel, L., George, K.H. & Arbizu, P.M. 2011. Submarine ridges do not prevent large-scale dispersal of abyssal fauna: A case study of *Mesocletodes* (Crustacea, Copepoda, Harpacticoida). *Deep Sea Research Part I: Oceanographic Research Papers*, **58**: 839–864.

Merritt, T.J.S., Shi, L., Chase, M.C., Rex, M.A., Etter, R.J. & Quattro, J.M. 1998. Universal Cytochrome b primers facilitate intraspecific studies in molluscan taxa. *Molecular Marine Biology and Biotechnology*, **7**: 7–11.

Messana, G., Argano, R. & Baldari, F. 1978. *Microcerberus* (Crustacea Isopoda Microcerberidea) from the Indian Ocean. *Monitore Zoologico Italiano*. Supplemento **10**: 69–79.

Millien-Parra, V. & Jaeger, J.J. 1999. Island biogeography of the Japanese terrestrial mammal assemblages: an example of a relict fauna. *Journal of Biogeography*, **26**: 959–972.

Moret, Y., Juchault, P. & Rigaud, T. 2001. *Wolbachia* endosymbiont responsible for cytoplasmic incompatibility in a terrestrial crustacean: effects in natural and foreign hosts. *Heredity*, **86**: 325–332.

Narita, S., Nomura, M., Kato, Y. & Fukatsu, T. 2006. Genetic structure of sibling butterfly species affected by *Wolbachia* infection sweep: evolutionary and biogeographical implications. *Molecular Ecology*, **15**: 1095–1108.

Nei, M. 1987. *Molecular evolutionary genetics*. Columbia University Press, New York.

Nunomura, N. 1973. Description of *Microcerberus kiiensis*, n. sp.: Primary record of the suborder Microcerberidea (Crustacea, Isopoda) in Japan. *Publications of the Seto Marine Biological Laboratory*, **21**: 87–93.

Pennak, R.W. 1958. A new micro-isopod from a Mexican marine beach. *Transactions of the American Microscopical Society*, **77**: 298–303.

Pfenninger, M. & Schwenk, K. 2007. Cryptic animal species are homogeneously distributed among taxa and biogeographical regions. *BMC Evolutionary Biology*, **7**: 121–127

Posada, D. 2003. Using MODELTEST and PAUP* to select a model of nucleotide substitution In: *Current protocols in bioinformatics* (A.D. Baxevanis, D.B. Davison, R.D.M. Page, G.A. Petsko, L.D. Stein & G.D. Stormo, eds.), pp. 6.5.1–6.5.14. John Wiley, New York.

Raimond, R., Marcadé, I., Bouchon, D., Rigaud, T., Bossy, J.P. & Souty-Grosset, C. 1999. Organization of the large mitochondrial genome in the isopod *Armadillidium vulgare*. *Genetics*, **151**: 203–210.

Raupach, M.J., Astrin, J.J., Hannig, K., Peters, M.K., Stoeckle, M.Y. & Wägele, J.W. 2010. Molecular species identification of Central European ground beetles (Coleoptera: Carabidae) using nuclear rDNA expansion segments and DNA barcodes. *Frontiers in Zoology*, **7**: 26–41.

Raupach, M.J., Barco, A., Steinke, D., Beermann, J., Laakmann, S., Mohrbeck, I., Neumann, H., Kihara, T.C., Pointner, K., Radulovici, A. & Segelken-Voigt, A. 2015. The application of DNA barcodes for the identification of marine crustaceans from the North Sea and adjacent regions. *PloS ONE*, **10**: e0139421.

Raupach, M.J., Bininda-Emonds, O.R., Knebelsberger, T., Laakmann, S., Pfaender, J. & Leese, F. 2014. Phylogeographical analysis of *Ligia oceanica* (Crustacea: Isopoda) reveals two deeply divergent mitochondrial lineages. *Biological Journal of the Linnean Society*, **112**: 16–30.

Raupach, M.J., Malyutina, M., Brandt, A. & Wägele, J.W. 2007. Molecular data reveal a highly diverse species flock within the munnopsoid deep-sea isopod *Betamorpha fusiformis* (Barnard, 1920) (Crustacea: Isopoda: Asellota) in the Southern Ocean. *Deep Sea Research II*, **54**: 1820–1830.

Richardson, H. 1912. Descriptions of a new genus of isopod crustaceans, and of two new species from South America. *Proceedings of the United States National Museum*, **43**: 201–204.

Riehl, T. & Brandt, A. 2010. Descriptions of two new species in the genus *Macrostylis* Sars, 1864 (Isopoda, Asellota, Macrostylidae) from the Weddell Sea (Southern Ocean), with a synonymisation of the genus *Desmostylis* Brandt, 1992 with *Macrostylis*. *Zookeys*, **57**: 9–49.

Riehl, T. & Kaiser, S. 2012. Conquered from the deep sea? A new deep-sea isopod species from the Antarctic shelf shows pattern of recent colonization. *PLoS ONE*, **7**: e49354.

Rigaud, T., Moreau, J. & Juchault, P. 1999. *Wolbachia* infection in the terrestrial isopod *Oniscus asellus*: sex ratio distortion and effect on fecundity. *Heredity*, **83**: 469–475.

Ronquist, F. & Huelsenbeck, J.P. 2003. MrBayes 3: Bayesian phylogenetic inference under mixed models. *Bioinformatics*, **19**: 1572–1574.

Ronquist, F., Teslenko, M., Van Der Mark, P., Ayres, D.L., Darling, A., Höhna, S., Larget, B., Liu, L., Suchard, M.A. & Huelsenbeck, J.P. 2012. MrBayes 3.2: efficient Bayesian phylogenetic inference and model choice across a large model space. *Systematic Biology*, **61**: 539–542.

Rozas, J. & Rozas, R. 1999. DnaSP version 3: an integrated program for molecular population genetics and molecular evolution analysis. *Bioinformatics*, **15**: 174–175.

Sars, G.O. 1864. Om en anomal Gruppe af Isopoder. *Forhandlinger i Videnskabs-Selskabet i Kristiania*, **1863**: 205–221.

Sars, G.O. 1909. Copepoda Harpacticoida. Parts XXVII & XXVIII. Cletodidae (concluded), Anchorabolidae, Cylindropsyllidae, Tachidiidae (part). *An Account of the Crustacea of Norway, with short descriptions and figures of all the species*, **Vol. 5**, pp. 305–336.

Shoemaker, D.D., Dyer, K.A., Ahrens, M., McAbee, K. & Jaenike, J. 2004. Decreased diversity but increased substitution rate in host mtDNA as a consequence of *Wolbachia* endosymbiont infection. *Genetics*, **168**: 2049–2058.

Shoemaker, D.D., Katju, V. & Jaenike, J. 1999. *Wolbachia* and the evolution of reproductive isolation between *Drosophila recens* and *Drosophila subquinaria*. *Evolution*, **53**: 1157–1164.

Shoemaker, D.D., Keller, G. & Ross, K.G. 2003. Effects of *Wolbachia* on mtDNA variation in two fire ant species. *Molecular Ecology*, **12**: 1757–1771.

Shoemaker, D.D., Ross, K.G., Keller, L., Vargo, E. & Werren, J.H. 2000. *Wolbachia* infections in native and introduced populations of fire ants *(Solenopsis* spp.). *Insect Molecular Biology*, **9**: 661–673.

Sket, B. 1960. Einige neue Formen der Malacostraca aus Jugoslawien III. *Bulletin Scientifique* (Belgrade), **5**: 73–75.

Stouthamer, R., Breeuwer, J.A. & Hurst, G.D. 1999. *Wolbachia pipientis*: microbial manipulator of arthropod reproduction. *Annual Reviews in Microbiology*, **53**: 71–102.

Tajima, F. 1983. Evolutionary relationship of DNA sequences in finite populations. *Genetics*, **105**: 437–460.

Tamura, K. & Nei, M. 1993. Estimation of the number of nucleotide substitutions in the control region of mitochondrial DNA in humans and chimpanzees. *Molecular Biology and Evolution*, **10**: 521–526.

Thompson, J.D., Higgins, D.G. & Gibson, T.J. 1994. CLUSTAL W: improving the sensitivity of progressive multiple sequence alignment through sequence weighting, position-specific gap penalties and weight matrix choice. *Nucleic Acids Research*, **22**: 4673–4680.

Varela, A.I. & Haye, P.A. 2012. The marine brooder *Excirolana braziliensis* (Crustacea: Isopoda) is also a complex of cryptic species on the coast of Chile. *Revista Chilena de Historia Natural*, **85**: 495–502.

Wägele, J.W. 1982. On a new *Microcerberus* from the Red Sea and the relationship of the Microcerberidea to the Anthuridea (Crustacea, Isopoda). *Zoologica Scripta*, **11**: 281–286.

Wägele, J.W. 1983. On the origin of the Microcerberidae (Crustacea: Isopoda). *Zeitschrift fuer Zoologische Systematik und Evolutionsforschung*, **21**: 249–262.

Wägele, J.W., Voelz, N.J. & McArthur, J. 1995. Older than the Atlantic Ocean: discovery of a fresh water *Microcerberus* (Isopoda) in North America and erection of *Coxicerberus*, new genus. *Journal of Crustacean Biology*, **15**: 733–745.

Xiao, J.H., Wang, N.X., Murphy, R.W., Cook, J., Jia, L.Y. & Huang, D.W. 2012. *Wolbachia* infection and dramatic intraspecific mitochondrial DNA divergence in a fig wasp. *Evolution*, **66**: 1907–1916.

Yamaoka, K., Nakagawa, T. & Uno, T. 1978. Application of Akaike's information criterion (AIC) in the evaluation of linear pharmacokinetic equations. *Journal of Pharmacokinetics and Pharmacodynamics*, **6**: 165–175.

Yin, J., Pan, D., He, C., Wang, A., Yan, J. & Sun, H. 2013. Morphological and molecular data confirm species assignment and dispersal of the genus *Ligia* (Crustacea: Isopoda: Ligiidae) along northeastern coastal China and East Asia. *Zoological Journal of the Linnean Society*, **169**: 362–376.

Zhou, W., Rousset, F. & O'Neill, S. 1998. Phylogeny and PCR-based classification of *Wolbachia* strains using wsp gene sequences. *Proceedings of the Royal Society of London, B: Biological Sciences*, **265**: 509–515.